CHEMISTRY OF MATERIALS

pubs.acs.org/cm

Methods/Protocols

Different Efforts but Similar Insights in Battery R&D: Electrochemical Impedance Spectroscopy *vs* Galvanostatic (Constant Current) Technique

Lukas Stolz, Miran Gaberšček, Martin Winter, and Johannes Kasnatscheew*

Cite This: *Chem. Mater.* 2022, 34, 10272−10278

Read Online

ACCESS | Metrics & More | Article Recommendations | Supporting Information

ABSTRACT: Electrochemical impedance spectroscopy (EIS) using *alternating currents* is a widely established technique to investigate kinetic aspects of batteries and their components, though it requires an interruption of battery operation with extra measurement time and effort. In this work, EIS is compared with the conventional galvanostatic (constant current) technique, which is based on *direct currents*, being the standard operation mode of batteries. Data from constant current measurements not only are representing application conditions but also are automatically and continuously generated during routine charge/discharge processes, *i.e.*, without *extra* measurement efforts, and do give kinetic insights via the characteristic overvoltage (= resistance-reasoned voltage rise/decrease), as well. In fact, distinguishing between even very similar values for ohmic (R_Ω), charge transfer (R_{ct}), and mass transport (R_{mt}) resistances can be done via analysis of overvoltage data from constant current measurements, as exemplarily demonstrated in symmetric Li||Li and $LiNi_{0.6}Mn_{0.2}Co_{0.2}O_2$ (NMC622)||Li cells with poly(ethylene oxide)-based solid polymer electrolyte, finally proving their validity. From a practical point of view, direct-current methods can be beneficial for R&D of kinetic aspects in batteries, as data is directly obtained and, thus, application-oriented.

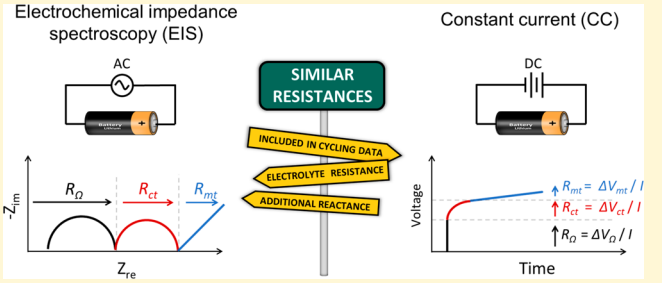

INTRODUCTION

The thermodynamically possible specific energy/energy density of batteries is practically limited during cell operations by resistance-induced overvoltages (polarizations), *i.e.*, ohmic- (R_Ω), activation- (charge transfer; R_{ct}), and concentration polarization (mass transport; R_{mt}), in particular at kinetically harsher conditions, *e.g.*, high rates and/or low temperatures.[1]

A common strategy to investigate and distinguish these resistance types is electrochemical impedance spectroscopy (EIS), either performed in *potentio-* (PEIS) or *galvano-* (GEIS) mode, *i.e.* with alternating current (AC) or alternating voltage excitations, respectively. The impedance can be obtained from the sinusoidal current and voltage relation, which contains both reactance and resistance values, illustrated in the imaginary and real parts (*y*- and *x*-axis) in the Nyquist plot, respectively.[2,3] The former are obtained from phase shifts between voltage/current curves and represent capacitive and/or inductive effects, while the latter are obtained from the voltage/current linear region and represent resistances.[4] Worth noting, the excitation in EIS must remain small (in the micro-ampere or millivolt region)[5] in order to remain a linear relation between voltage and current, being an essential requirement for accurate estimation of R_Ω, R_{ct}, and R_{mt} values according ohmic law, as schematically shown in Figure 1.[6]

The main focus of AC based EIS in battery R&D is the determination of electronic and/or ionic conductivities of electrodes, electrolytes, interphases, and interfaces, also providing information with respect to reactance, *e.g.*, capacitance. Batteries are operated with *direct currents* (DC), where resistance values have more relevance, suggesting DC-based methods are more application-oriented.

The current excitation in GEIS can be theoretically also mimicked by DC steps (Figure 2) and, therefore, is a reasonable mode for the comparison purposes in this work. From a practical point of view, solid-state batteries (SSBs) with solid polymer electrolytes (SPEs) are suitable for kinetic investigations due to their poor ion transport kinetics compared to liquid-based conventional batteries, allowing clear distinguishing of resistances under experimentally convenient conditions, *i.e.*, moderate currents/rates and temperature.[7−11]

In this work, a poly(ethylene oxide) (PEO)-based solid polymer electrolyte (SPE) is investigated, compared and validated in Li||Li and $LiNi_{0.6}Mn_{0.2}Co_{0.2}O_2$ (NMC622)||Li metal battery cells[12−16] via AC and DC modes. Both the

Received: August 3, 2022
Revised: November 7, 2022
Published: December 2, 2022

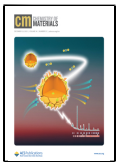

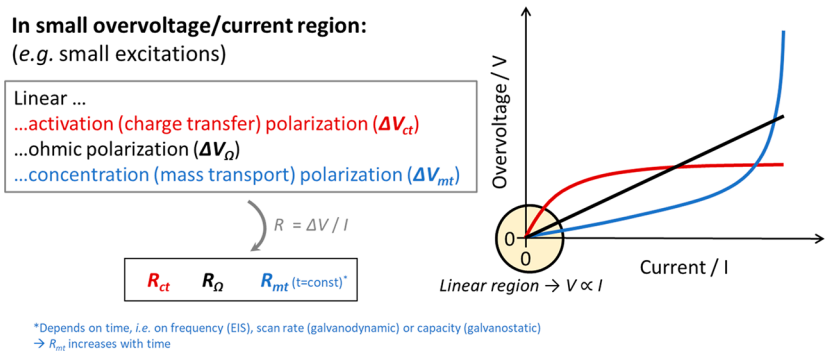

Figure 1. Current (or voltage) excitation in EIS is generally kept small in order to have a linear relation of overvoltage and current for each polarization type, being a fundamental basis to accurately determine the resistance types according to ohmic law.

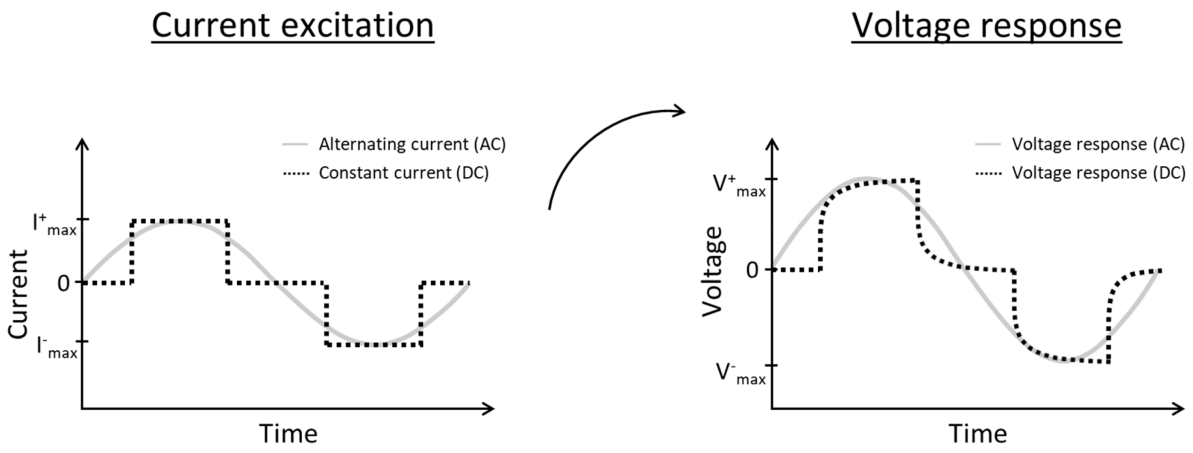

Figure 2. Schematic comparison between AC and DC excitations with the corresponding voltage responses. The sinusoidal current excitation of GEIS can be mimicked by constant current steps demonstrating fundamental similarities.

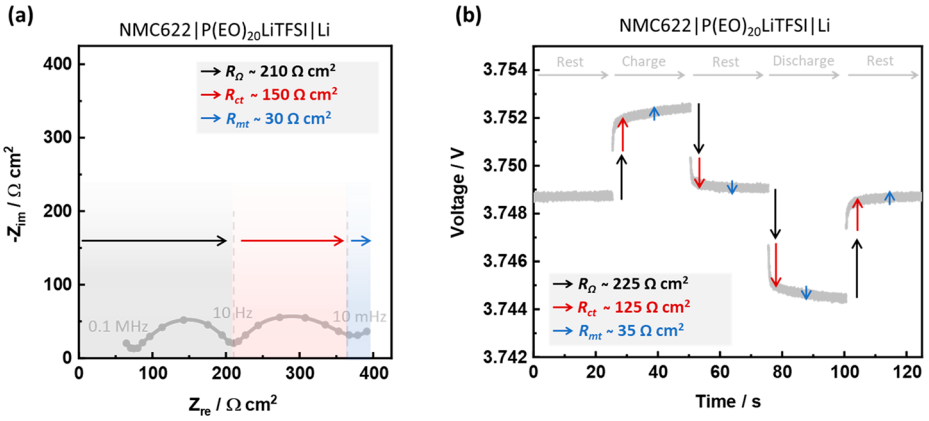

Figure 3. (a) Nyquist plot obtained by EIS measurement of a NMC622|$P(EO)_{20}$LiTFSI|Li cell at 60 °C, measured in a frequency range between 0.1 MHz and 10 mHz and with an applied current density amplitude of 10 μA cm^{-2}. (b) Voltage−time plot of a DC experiment of a NMC622|$P(EO)_{20}$LiTFSI|Li cell at 60 °C, with resting steps between positive and negative current excitation, each with a current density of 10 μA cm^{-2} for 25 s. Both techniques reveal similar values for the respective resistances.

relevance of R_Ω, R_{ct}, and R_{mt} themselves as well as the practical benefits of automatically generated voltage profiles via DC mode are highlighted and discussed, finally demonstrating the effectiveness of galvanostatic techniques for battery cell behavior analysis.

EXPERIMENTAL SECTION

a. Materials. Poly(ethylene oxide) (PEO, MW 300 000 Da), 99.5%) was purchased from Sigma-Aldrich, Germany. Lithium bis(trifluoromethanesulfonyl)imide (LiTFSI, 99.9%) was purchased from Solvay, France. $LiNi_{0.6}Mn_{0.2}Co_{0.2}O_2$ (NMC622) electrodes (1 mAh cm^{-2}) were purchased from Customcells, Germany. Lithium metal (Albemarle) was purchased from Albemarle, U.S.A. Polyvinyl chloride (PVC) foil (400 μm thickness) was purchased from CreativDiscount, Germany. Material storage and sample preparations were performed in a dry room with a dew point of −65 °C. The NMC622 sheets were punched into discs with 14 mm

https://doi.org/10.1021/acs.chemmater.2c02376
Chem. Mater. 2022, 34, 10272−10278

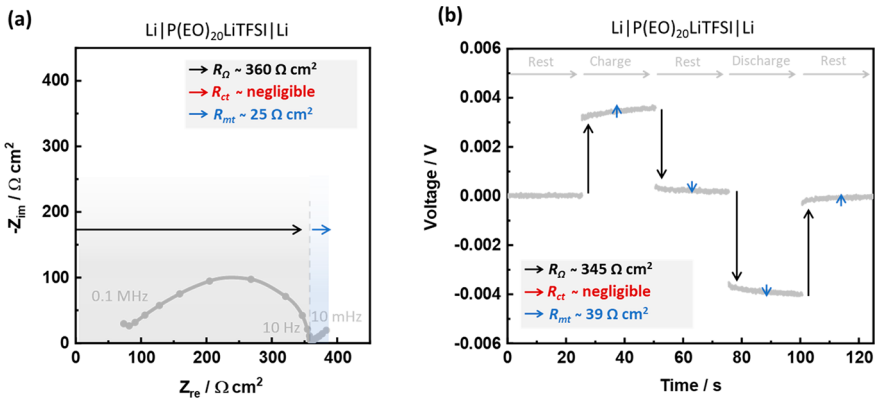

Figure 4. (a) Nyquist plot obtained by EIS measurement of a Li|P(EO)$_{20}$LiTFSI|Li cell at 60 °C, measured in a frequency between 0.1 MHz and 10 mHz and with an applied current density amplitude of 10 μA cm^{-2}. (b) Voltage−time plot of a DC experiment in a Li|P(EO)$_{20}$LiTFSI|Li cell at 60 °C, with resting steps between positive and negative current excitations, each with a current density of 10 μA cm^{-2} for 25 s. Both techniques provide very similar values for the respective resistances.

diameter and dried at 120 °C under a vacuum of 10^{-7} mbar overnight. PEO was dried under a vacuum of 10^{-7} mbar at 45 °C and LiTFSI at 110 °C for 2 days before use.

b. SPE Membrane Preparation. PEO-based SPE polymer membranes were prepared by dry mixing PEO and LiTFSI with a molar ratio of 20:1 (EO:Li). The obtained mixture was stored in a pouch bag under vacuum overnight (60 °C).[17] The resulting gum-like material was sandwiched between Mylar foil sheets and pressed at 100 °C with an applied pressure of 15 bar for 10 min.

c. Cell Assembly. The cells (coin cell configuration) were assembled using the polymer membranes with 12 mm diameter and 400 μm thickness inside rings of PVC foil with 16 mm outer diameter and 12 mm inner diameter and sandwiched between a lithium metal electrode (15 mm diameter, but with an effective area of only 12 mm due to 12 mm SPE diameter) and a NMC 622 electrode (12 mm diameter) and/or between a second lithium metal electrode in the case of a symmetric cell configuration.

d. Constant Current Measurements. All constant current cycling experiments were conducted on a Arbin Instruments battery cell test system at 60 °C in a climate chamber (Memmert). The used current densities are mentioned in the figure captions.

e. Electrochemical Impedance Spectroscopy (EIS). EIS measurements were conducted utilizing an Arbin Instruments battery cell test system with a Gamry Instruments Interface 5000 potentiostat. The measurements were performed in the frequency range of 0.1 MHz to 10 mHz with an applied current density amplitude of 10 μA cm^{-2}. The temperature (60 °C) was controlled using a climate chamber (Memmert).

RESULTS AND DISCUSSION

A typical Nyquist plot of an $LiNi_{0.6}Mn_{0.2}Co_{0.2}O_2$ (NMC622)|| Li cell obtained via electrochemical impedance spectroscopy (EIS) with poly(ethylene oxide)-based solid polymer electrolyte (PEO-based SPE) is depicted in Figure 3a.

According to the literature consensus, the *x*-axis minimum at high frequency corresponds to the bulk electrolyte resistance (here 80 Ω cm^2), followed by a semicircle that is attributed to the interphase resistance.[18] Both together contribute to the ohmic resistance of the cell (R_Ω; here 210 Ω cm^2). The second semicircle represents the charge transfer resistance (R_{ct}), also assigned to activation polarization, according to the Butler−Volmer equation (here 150 Ω cm^2).[2] The "tail" at very low frequency (<1 Hz) results from mass transport limitations (R_{mt}; here 30 Ω cm^2) and is in particular observable for poor conducting electrolytes. In this context, it needs to be noted that considering only the real part of the low frequency region should be regarded as an estimation of the actual mass transfer resistance, as capacitive effects, *e.g.*, formation of a double layer, are neglected. While the impedances of the ohmic and charge transfer processes are already relaxed to predominantly resistive contributions (represented by semicircles with a Z_{re}-axis intercept), the mass transport "tail" is not and is composed of resistive and capacitive contributions. Here, the more precise way is to introduce the absolute value of the low frequency impedance ($Z_{abs,mt}$). However, in this work, possible capacitive contributions are neglected as the error is small within the investigated battery cell (low mass transport contribution compared to ohmic and charge transfer resistances) and is calculated to be below 3% (Figure S1, Supporting Information).

In contrast, Figure 3b depicts a galvanostatic, *i.e.*, direct current (DC), approach for an identical cell. While the Nyquist plot directly indicates the resistance values from the *x*-axis data of the resulting curves, the resistances obtained by DC measurements need to be calculated from the overvoltages (ΔV) and the applied current according to ohmic law.[19] The value of R_Ω can be related with the *iR*-drop, which is known as a sudden change in cell voltage immediately after abrupt changes in current, and amounts here to 225 Ω cm^2, as shown in Figure 3b. For a given current this type of overvoltage occurs immediately simply according ohmic law.[19] The other resistance requires some (short) time, *i.e.*, activation/charge transfer (R_{ct}) and (afterward) formation of a concentration gradient in the course of mass-transport limitation/concentration polarization (R_{mt}), thus occuring after ohmic drop.[19] The value for R_{ct} can be obtained from the subsequent (first milliseconds after abrupt current change) "activation" overvoltage, thus is attributed to the second-type overvoltage in the curve, and amounts to 125 Ω cm^2. Afterward, the continuous increase in overvoltage can be attributed to concentration polarization, thus to R_{mt} (35 Ω cm^2), being the third-type overvoltage in the voltage curve.[19] For a fair comparison with respect to R_{mt}, the durations of DC charge and discharge amount to 25 s, which mimics the charge (*i.e.*, the quarter) of the sinusoidal curve from the AC experiment of 10 mHz (=

https://doi.org/10.1021/acs.chemmater.2c02376
Chem. Mater. 2022, 34, 10272−10278

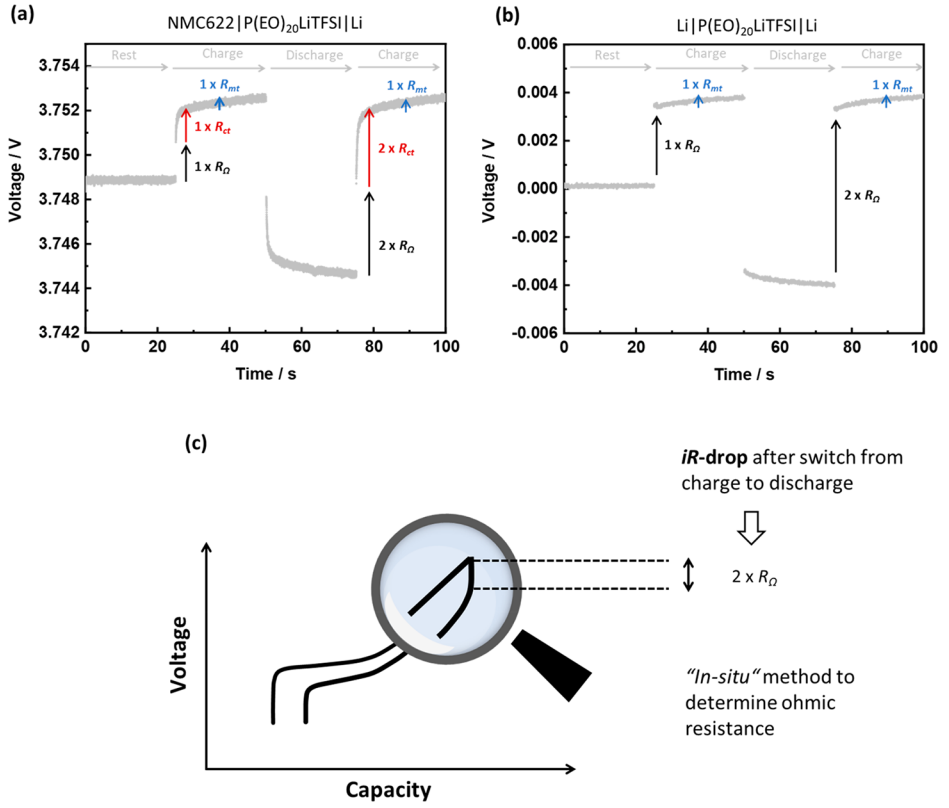

Figure 5. (a) Voltage−time plot of a DC experiment in NMC622|P(EO)$_{20}$LiTFSI|Li cell and (b) Li|P(EO)$_{20}$LiTFSI|Li cell at 60 °C with a current density of 10 μA cm^{-2} for 25 s for charge and discharge. Switching the current from charge to discharge (without a resting step) results in an *iR*-drop that reflects twice the R_Ω of the cell, as schematically illustrated in (c), while R_{mt} remains unaffected as it is (only relevant in a longer-time frame, R_{ct} doubles as well in the NMC622||Li cell).

100 s for one total wave), as schematically shown in Figure 2. In fact, the respective resistances of the DC method are in the same range as obtained from EIS.

Indeed, assigning the battery circuit diagram and fitting could further increase the precision of the respective resistance values in the Nyquist plot; however, this is an additional effort, and such assignments can get complex and frequently can even lead to misinterpretations.[2,3] Moreover, in this study, the aim is to simply show the obvious similarity with respect to the resistance (R_Ω, R_{ct}, R_{mt}) values of both methods; worth noting, with or without fitting efforts and by neglecting capacitive contributions (Figure S1), the total sums of the resistances (EIS method: 390 Ω cm^2; DC method: 385 Ω cm^2) are similar, finally demonstrating a reasonable similarity and comparability of these methods.

For a validity check, the comparison between EIS and DC data is also applied in a symmetric Li||Li cell (Figure 4). Again, both techniques provide similar values for the respective resistances. The second semicircle in the medium frequency region, related with R_{ct}, is absent in the Nyquist plot, which is in line with the literature.[18] Moreover, compared to an NMC622-based cell, R_Ω of the symmetric Li cell is higher (360 *vs* 210 Ω cm^2) and can be attributed to an additional interphase resistance of Li. Subtracting the electrolyte resistance of 80 Ω cm^2 from R_Ω (Figure 3a), the interphase resistance is 280 Ω cm^2 in the Li||Li cell and 130 Ω cm^2 in the NMC622||Li cell, respectively. This outcome suggests the Li interphase, probably pronounced via solid electrolyte interphase (SEI) on Li, is the predominant contribution to R_Ω of the cell and is approximately doubled in the Li||Li cell. Again, also R_{mt} is in a similar range as observed in EIS and independent of the applied electrochemical technique and the cell setup as well as the sum of the resistances (EIS method: 385 Ω cm^2; DC method: 384 Ω cm^2).

Worth noting, the DC method can separate the three resistances R_Ω, R_{ct}, and R_{mt}, but it cannot separate R_Ω into the electrolyte resistance and interphase resistance, rendering EIS a better choice for this particular case.

Theoretically, only if the interphase resistance is absent, the first *x*-axis intercept (in this case, the first minimum of the EIS curve) of the Nyquist plot can be attributed to R_Ω, but this is not common in lithium-based battery cells as interphases are omnipresent on both anodes and cathodes.[20−23] For diagnostic efforts within R&D, a clear attribution of the respective semicircles to resistances in the EIS spectrum is mandatory; otherwise, this can lead to misleading conclusions,[2,3,24] rendering literature interpretation based on EIS difficult.

In the case of a constant current charge/discharge experiment without resting times in between, the *iR*-drop is twice as much as R_Ω of the cell, as exemplarily demonstrated for a NMC622|P(EO)$_{20}$LiTFSI|Li cell in Figure 5a as well as for a Li|P(EO)$_{20}$LiTFSI|Li symmetric cell in Figure 5b. Also, the activation overvoltage doubles, *i.e.*, doubles the R_{ct}. This can be explained by the switch from positive to negative currents (and *vice versa*), which results in a doubling of the current magnitude and R_Ω and R_{ct} appearing in a short time scale. In contrast, R_{mt} remains similar after switching from charge to discharge (and *vice versa*) as the formed concentration gradients during discharge require an identical time to be neutralized in the subsequent charge process, before

https://doi.org/10.1021/acs.chemmater.2c02376
Chem. Mater. 2022, 34, 10272−10278

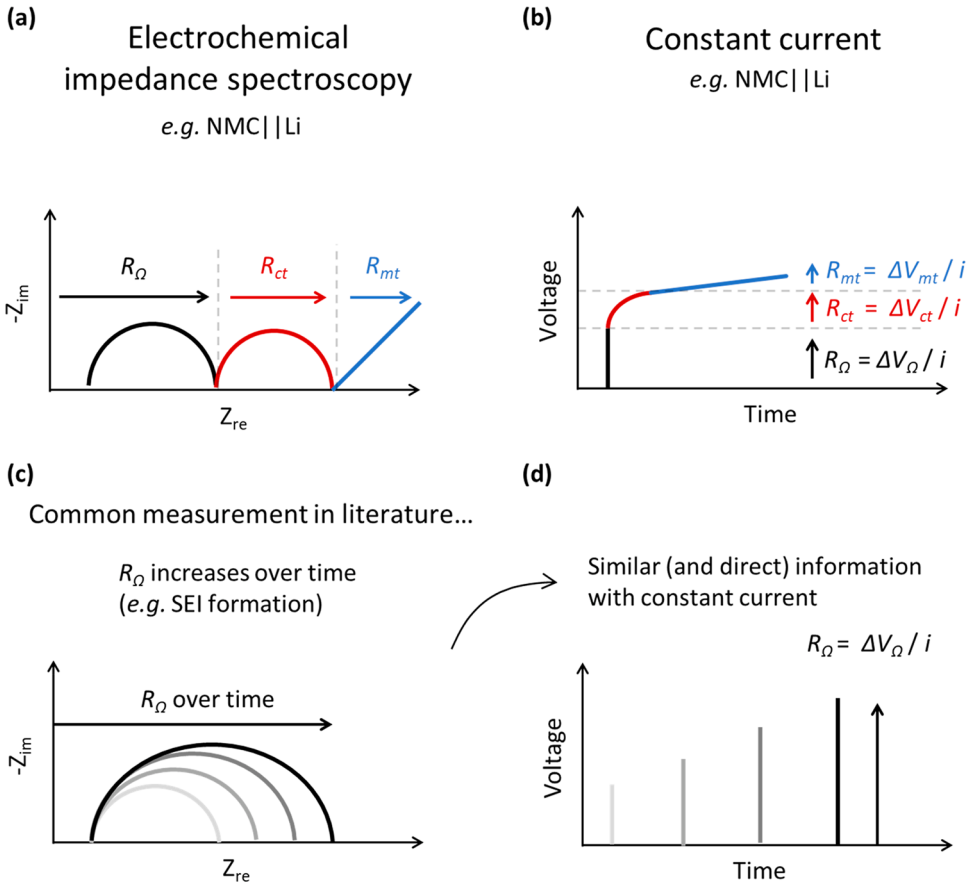

Figure 6. Comparison between the (a) EIS and (b) DC, *e.g.* constant current techniques, with respect to R_Ω, R_{ct}, and R_{mt} determination in batteries. Both methods can observe the respective resistances and even provide similar values. Nevertheless, in this case DC can be considered as more pragmatic and reasonable ("*in situ*") as no interruption in battery operation, and *extra* measurement efforts and time are necessary. Even specific experiments, *e.g.* SEI aging, where the evolution of R_Ω is observed during a defined measurement duration (c) is also possible with DC method (d), which generates data directly.

building up a concentration gradient in the opposite direction (Figure 5).

An NMC622-reasoned voltage increase via delithiation/lithiation during charge/discharge[25−28] can be reasonably ignored in the short time frame of 25 s and, thus, can be predominantly attributed to an R_{mt}-reasoned overvoltage. This conclusion is supported by the observation of a similar overvoltage also in Li||Li cells, shown in Figure 5b.

The DC technique can be regarded as a pragmatic method, where resistance values can be deduced directly from the galvanostatic data, thus, quasi-"*in situ*", independent of excitation of any criteria (Figure 1). In particular, this is a powerful technique to precisely determine R_Ω (simply via the *i*R-drop), shown in Figure 5c, as there is no need to interrupt battery operation, contrary to the EIS technique, and no need for modeling and fitting, rendering clear interpretations. Also, R_{ct} and R_{mt} can be obtained from DC data, while EIS measurements require additional effort and time, in particular because of the application of low frequencies in the mHz regime, which are necessary to obtain R_{ct} and R_{mt}.

CONCLUSIONS

This work compares electrochemical impedance spectroscopy (EIS), based on alternating current (AC), with galvanostatic technique, based on direct current (DC), in terms of the three resistances, *i.e.*, ohmic (R_Ω), charge transfer (R_{ct}), and mass transport (R_{mt}) resistance in solid-state batteries with a poly(ethylene oxide)-based solid polymer electrolyte.

In fact, both techniques, under the conditions of (very) small excitation signal, are able to observe these resistances and reveal even similar values, as demonstrated in Li-$Ni_{0.6}Mn_{0.2}Co_{0.2}O_2$ (NMC622)||Li and Li||Li cells (Figure 6). However, compared to EIS, the DC measurements can be advantageous as they automatically generate data during battery operation, *i.e.*, without interruption and additional experimental efforts, *e.g.*, the availability of a potentiostat, and *extra* measurement time, in particular for the low frequency part of the measurement, which is necessary to obtain R_{ct} and R_{mt}. Worth noting, EIS is generally performed under impractical low current excitations to meet the criterion of linearity (Figure 1). This can mislead in terms of the interpretation of the actual relevant battery resistances under more practical, *i.e.*, higher, currents. For example, the value of the charge transfer resistance can become relatively low (compared to total resistance), when the applied currents are higher and beyond the linear current−voltage region (Figure 1). In this case, data from the EIS technique can over-emphasize this particular resistance type.

Moreover, the EIS technique can have plenty of freedom in interpretation, which increases the risk of misinterpretation[2,3] and, as shown here, can be validated and proven via DC techniques and *vice versa*.

https://doi.org/10.1021/acs.chemmater.2c02376
Chem. Mater. 2022, 34, 10272−10278

Data for specific processes like aging experiments, which are commonly investigated by means of EIS via observing R_Ω over time in the course of, *e.g.*, growth of the solid electrolyte interphase (SEI),[29−31] can be also obtained by DC experiments, as illustrated in Figure 6c,d, respectively.

Nevertheless, EIS is a precious method as it reveals additional data (reactance) for more in-depth scientific questions and is able to distinguish between different types of ohmic resistances at high frequency mode, *i.e.*, distinguishing the resistances from electrolyte and SEI;[32−35] it consequently remains a suitable method to determine electrolyte conductivity.

■ ASSOCIATED CONTENT

Supporting Information

The Supporting Information is available free of charge at https://pubs.acs.org/doi/10.1021/acs.chemmater.2c02376.

Calculation of the error due to the simplifications within evaluation of resistance/impedance from galvanostatic measurement (PDF)

■ AUTHOR INFORMATION

Corresponding Author

Johannes Kasnatscheew − *Helmholtz-Institute Münster, IEK-12, Forschungszentrum Jülich GmbH, 48149 Münster, Germany*; orcid.org/0000-0002-8885-8591; Email: j.kasnatscheew@fz-juelich.de

Authors

Lukas Stolz − *Helmholtz-Institute Münster, IEK-12, Forschungszentrum Jülich GmbH, 48149 Münster, Germany*

Miran Gaberščček − *Department of Materials Chemistry, National Institute of Chemistry, 1000 Ljubljana, Slovenia*; orcid.org/0000-0002-8104-1693

Martin Winter − *Helmholtz-Institute Münster, IEK-12, Forschungszentrum Jülich GmbH, 48149 Münster, Germany; MEET Battery Research Center, Institute of Physical Chemistry, University of Münster, 48149 Münster, Germany*

Complete contact information is available at: https://pubs.acs.org/10.1021/acs.chemmater.2c02376

Notes

The authors declare no competing financial interest.

■ ACKNOWLEDGMENTS

Financial support from the German Federal Ministry for Education and Research (BMBF) within the project, MEET Hi-End III (03XP0258A) as part of the ExcellBattMat Cluster, is gratefully acknowledged.

■ REFERENCES

(1) Weiss, M.; Ruess, R.; Kasnatscheew, J.; Levartovsky, Y.; Levy, N. R.; Minnmann, P.; Stolz, L.; Waldmann, T.; Wohlfahrt-Mehrens, M.; Aurbach, D.; Winter, M.; Ein-Eli, Y.; Janek, J. Fast Charging of Lithium-Ion Batteries: A Review of Materials Aspects. *Adv. Energy Mater.* **2021**, *11* (33), 2101126.

(2) Mei, B.-A.; Lau, J.; Lin, T.; Tolbert, S. H.; Dunn, B. S.; Pilon, L. Physical Interpretations of Electrochemical Impedance Spectroscopy of Redox Active Electrodes for Electrical Energy Storage. *J. Phys. Chem. C* **2018**, *122* (43), 24499−24511.

(3) Mei, B.-A.; Munteshari, O.; Lau, J.; Dunn, B.; Pilon, L. Physical Interpretations of Nyquist Plots for EDLC Electrodes and Devices. *J. Phys. Chem. C* **2018**, *122* (1), 194−206.

(4) Pilla, A. A. A Transient Impedance Technique for the Study of Electrode Kinetics. *J. Electrochem. Soc.* **1970**, *117* (4), 467.

(5) Zsigmond, A.; Libich, J. Testing of a Prototype Device Using Electrochemical Impedance Spectroscopy (EIS) Method. *ECS Trans.* **2020**, *99* (1), 391−400.

(6) Bard, A. J.; Faulkner, L. R. *Electrochemical Methods: Fundamentals and Applications*; Wiley: 2001.

(7) Kasnatscheew, J.; Rodehorst, U.; Streipert, B.; Wiemers-Meyer, S.; Jakelski, R.; Wagner, R.; Laskovic, I. C.; Winter, M. Learning from Overpotentials in Lithium Ion Batteries: A Case Study on the $LiNi_{1/3}Co_{1/3}Mn_{1/3}O_2$ (NCM) Cathode. *J. Electrochem. Soc.* **2016**, *163* (14), A2943−A2950.

(8) Homann, G.; Stolz, L.; Neuhaus, K.; Winter, M.; Kasnatscheew, J. Effective Optimization of High Voltage Solid-State Lithium Batteries by Using Poly(ethylene oxide)-Based Polymer Electrolyte with Semi-Interpenetrating Network. *Adv. Funct. Mater.* **2020**, *30* (46), 2006289.

(9) Homann, G.; Stolz, L.; Winter, M.; Kasnatscheew, J. Elimination of "Voltage Noise" of Poly (Ethylene Oxide)-Based Solid Electrolytes in High-Voltage Lithium Batteries: Linear versus Network Polymers. *iScience* **2020**, *23* (6), 101225.

(10) Homann, G.; Meister, P.; Stolz, L.; Brinkmann, J. P.; Kulisch, J.; Adermann, T.; Winter, M.; Kasnatscheew, J. High-Voltage All-Solid-State Lithium Battery with Sulfide-Based Electrolyte: Challenges for the Construction of a Bipolar Multicell Stack and How to Overcome Them. *ACS Applied Energy Materials* **2020**, *3* (4), 3162−3168.

(11) Stolz, L.; Hochstädt, S.; Röser, S.; Hansen, M. R.; Winter, M.; Kasnatscheew, J. Single-Ion versus Dual-Ion Conducting Electrolytes: The Relevance of Concentration Polarization in Solid-State Batteries. *ACS Appl. Mater. Interfaces* **2022**, *14* (9), 11559−11566.

(12) Stolz, L.; Homann, G.; Winter, M.; Kasnatscheew, J. Area Oversizing of Lithium Metal Electrodes in Solid-State Batteries: Relevance for Overvoltage and thus Performance? *ChemSusChem* **2021**, *14* (10), 2163−2169.

(13) Stolz, L.; Homann, G.; Winter, M.; Kasnatscheew, J. Kinetical Threshold Limits in Solid-State Lithium Batteries: Data on Practical Relevance of Sand Equation. *Data in Brief* **2021**, *34*, 106688.

(14) Stolz, L.; Röser, S.; Homann, G.; Winter, M.; Kasnatscheew, J. Pragmatic Approaches to Correlate between the Physicochemical Properties of a Linear Poly(ethylene oxide)-Based Solid Polymer Electrolyte and the Performance in a High-Voltage Li-Metal Battery. *J. Phys. Chem. C* **2021**, *125* (33), 18089−18097.

(15) Stolz, L.; Homann, G.; Winter, M.; Kasnatscheew, J. Realizing Poly(ethylene oxide) as a Polymer for Solid Electrolytes in High Voltage Lithium Batteries via Simple Modification of the Cell Setup. *Materials Advances* **2021**, *2* (10), 3251−3256.

(16) Stolz, L.; Homann, G.; Winter, M.; Kasnatscheew, J. The Sand Equation and its Enormous Practical Relevance for Solid-State Lithium Metal Batteries. *Mater. Today* **2021**, *44*, 9−14.

(17) Homann, G.; Stolz, L.; Nair, J.; Laskovic, I. C.; Winter, M.; Kasnatscheew, J. Poly(Ethylene Oxide)-based Electrolyte for Solid-State-Lithium-Batteries with High Voltage Positive Electrodes: Evaluating the Role of Electrolyte Oxidation in Rapid Cell Failure. *Sci. Rep* **2020**, *10* (1), 4390.

(18) Fauteux, D. Formation of a passivating film at the lithium-PEO-LiCF3SO3 interface. *Solid State Ion.* **1985**, *17* (2), 133−138.

(19) Winter, M.; Brodd, R. J. What are batteries, fuel cells, and supercapacitors? *Chem. Rev.* **2004**, *104* (10), 4245−4269.

(20) Kasnatscheew, J.; Placke, T.; Streipert, B.; Rothermel, S.; Wagner, R.; Meister, P.; Laskovic, I. C.; Winter, M. A Tutorial into Practical Capacity and Mass Balancing of Lithium Ion Batteries. *J. Electrochem. Soc.* **2017**, *164* (12), A2479−A2486.

(21) Kasnatscheew, J.; Streipert, B.; Röser, S.; Wagner, R.; Cekic Laskovic, I.; Winter, M. Determining Oxidative Stability of Battery Electrolytes: Validity of Common Electrochemical Stability Window (ESW) Data and alternative Strategies. *Phys. Chem. Chem. Phys.* **2017**, *19* (24), 16078−16086.

(22) Kasnatscheew, J.; Evertz, M.; Streipert, B.; Wagner, R.; Klopsch, R.; Vortmann, B.; Hahn, H.; Nowak, S.; Amereller, M.; Gentschev, A.

C.; Lamp, P.; Winter, M. The Truth about the 1st Cycle Coulombic Efficiency of $LiNi_{1/3}Co_{1/3}Mn_{1/3}O_2$ (NCM) Cathodes. *Phys. Chem. Chem. Phys.* **2016**, *18* (5), 3956−3965.
(23) Kasnatscheew, J.; Evertz, M.; Streipert, B.; Wagner, R.; Nowak, S.; Cekic Laskovic, I.; Winter, M. Changing Established Belief on Capacity Fade Mechanisms: Thorough Investigation of $LiNi_{1/3}Co_{1/3}Mn_{1/3}O_2$ (NCM111) under High Voltage Conditions. *J. Phys. Chem. C* **2017**, *121* (3), 1521−1529.
(24) Saidani, F.; Hutter, F. X.; Scurtu, R. G.; Braunwarth, W.; Burghartz, J. N. Lithium-ion battery models: a comparative study and a model-based powerline communication. *Adv. Radio Sci.* **2017**, *15*, 83−91.
(25) Kasnatscheew, J.; Röser, S.; Börner, M.; Winter, M. Do Increased Ni Contents in $LiNi_xMn_yCo_zO_2$ (NMC) Electrodes Decrease Structural and Thermal Stability of Li Ion Batteries? A Thorough Look by Consideration of the Li^+ Extraction Ratio. *ACS Applied Energy Materials* **2019**, *2* (11), 7733−7737.
(26) Kasnatscheew, J.; Evertz, M.; Kloepsch, R.; Streipert, B.; Wagner, R.; Cekic Laskovic, I.; Winter, M. Learning from Electrochemical Data: Simple Evaluation and Classification of $LiMO_2$-type-based Positive Electrodes for Li-Ion Batteries. *Energy Technology* **2017**, *5* (9), 1670−1679.
(27) Kasnatscheew, J.; Evertz, M.; Streipert, B.; Wagner, R.; Nowak, S.; Cekic Laskovic, I.; Winter, M. Improving Cycle Life of Layered Lithium Transition Metal Oxide ($LiMO_2$) based Positive Electrodes for Li Ion Batteries by Smart Selection of the Electrochemical Charge Conditions. *J. Power Sources* **2017**, *359*, 458−467.
(28) Kasnatscheew, J.; Wagner, R.; Winter, M.; Cekic-Laskovic, I. Interfaces and Materials in Lithium Ion Batteries: Challenges for Theoretical Electrochemistry. *Topics in Current Chemistry* **2018**, *376* (3), 16.
(29) Zhang, S. S.; Tran, D. T. A simple approach for superior performance of lithium/sulphur batteries modified with a gel polymer electrolyte. *J. Mater. Chem. A* **2014**, *2* (20), 7383−7388.
(30) Li, M.; Yang, B.; Zhang, Z.; Wang, L.; Zhang, Y. Polymer gel electrolytes containing sulfur-based ionic liquids in lithium battery applications at room temperature. *J. Appl. Electrochem.* **2013**, *43* (5), 515−521.
(31) Lu, Y.; Gu, S.; Hong, X.; Rui, K.; Huang, X.; Jin, J.; Chen, C.; Yang, J.; Wen, Z. Pre-modified Li3PS4 based interphase for lithium anode towards high-performance Li-S battery. *Energy Storage Mater.* **2018**, *11*, 16−23.
(32) Bruce, P. G.; Evans, J.; Vincent, C. A. Conductivity and Transference Number Measurements on Polymer Electrolytes. *Solid State Ion.* **1988**, *28*, 918−922.
(33) Zhang, S. S.; Xu, K.; Jow, T. R. EIS study on the formation of solid electrolyte. *Electrochim. Acta* **2006**, *51* (8−9), 1636−1640.
(34) Zhang, S. S.; Xu, K.; Jow, T. R. Electrochemical impedance study on the low temperature of Li-ion batteries. *Electrochim. Acta* **2004**, *49* (7), 1057−1061.
(35) Churikov, A. V. Transfer mechanism in solid-electrolyte layers on lithium: influence of temperature and polarization. *Electrochim. Acta* **2001**, *46* (15), 2415−2426.

https://doi.org/10.1021/acs.chemmater.2c02376
Chem. Mater. 2022, 34, 10272−10278